

Crack-bridging Bonding in Trivalent Chromium Composite Coatings on Pure Aluminum Using Carbon Nanotubes for Wear Resistance

E. Khodadad, M. K. Lei*

Surface Engineering Laboratory, School of Materials Science and Engineering, Dalian University of Technology, Dalian 116024, China

*E-mail: mklei@dlut.edu.cn

Received: 28 December 2013 / Accepted: 26 February 2014 / Published: 23 March 2014

The trivalent chromium composite coatings with multiwall carbon nanotubes (MWCNTs) were fabricated by the direct current deposition under an ultrasonic agitation on the pure aluminum substrate using a zincate interlayer. Compared with the trivalent chromium coatings, the chromium composite coatings about 35 μm thick with MWCNTs have the similar amorphous microstructure with a limited crystallization. The horizontal stymie of carbon nanotubes between the chromium grains was mainly located in the chromium composite coatings. A slightly increased microhardness to $\text{HV}_{1\text{N}}$ 9.2-9.8 GPa was obtained from $\text{HV}_{1\text{N}}$ 8.0-8.3 GPa of the pure chromium coatings. During the tribological test on a ball-on-disc tribometer against an Si_3N_4 ceramic counterface under a normal load of 0.5-2 N, the similar friction coefficient of the two trivalent chromium coatings changed in 0.60-0.47, which was dependent on the applied normal load. However, the significant increase in wear resistance of the chromium composite coatings with MWCNTs, relative to that of the pure chromium coatings, was found with the specific wear rate decreased by about 30-40 % under the applied normal load. A crack-bridging bonding model was proposed to explore the improvement mechanism in wear resistance by the carbon nanotubes as reinforced nanometer fiber in the trivalent chromium composite coatings.

Keywords: Trivalent chromium composite coatings; Carbon nanotubes; Direct current deposition; Crack-bridging bonding; Wear resistance

1. INTRODUCTION

The chromium electroplating plays an important role to increase the mechanical and chemical properties of aluminum and its alloys [1-3], but the chromium coatings are deposited on base of chromic acid solutions containing highly toxic compounds of hexavalent chromium. Environmental

consideration is responsible for increased interests to less toxic trivalent chromium baths as an eco-friendly alternative to hexavalent chromium baths. Unfortunately, the trivalent chromium electroplating on base of chloride chromium salt solutions usually has various microcracks on the hard chromium surface, and it is related to naturally microporous morphology [4]. Formation of the microcracks at the surface is the first sign of failure of chromium coatings, particularly along the sides of the indenter trace during tribological test. Therewith the cracks growth perpendicular to the scratch direction occurred with increasing the applied load [5]. Giovanardi and Orlando [6] reported that the presence of microcracks increased the brittleness, although the internal stress of the chromium coatings was decreased. Various attempts have been made to improve the mechanical properties of the trivalent chromium coatings. Zhang et al. [7, 8] found that with an annealing of the trivalent chromium coatings, the wear resistance was improved in comparison with that for the conventional chromium coatings, because the hard participation phases during the annealing can block the relative motion between crystal grains. However, the change of phase structure also led to the appearance of microcracks. The thick trivalent chromium coatings are more difficult to deposit, when the deposition rate is decreased sufficiently after several minutes due to use of such special complex agents to prevent the defects. Moreover, the trivalent chromium coatings relative the hexavalent chromium coatings have a lower hardness from their amorphous and/or nanocrystalline microstructure [9].

The carbon nanotubes (CNTs) as reinforced nanometer fiber in the composite exhibit the excellent enhanced properties, such as increased mechanical properties, corrosion resistance, electrical properties, as well as thermal conductivity and absorbability [10]. Recently, Zeng et al. [11-13] reported the distinct improvement in wear properties of the trivalent chromium coatings introduced by multiwall carbon nanotubes (MWCNTs), which is attributed to the fiber reinforcement effects of carbon nanotubes. However, the wear resistance mechanism of carbon nanotubes in the chromium composite coatings are not fully understood due to lack of systemically study of the reinforcement effects. The wear behavior of the trivalent chromium composite coatings with the intrinsic defects as microcracks is not clear.

In this paper, the surface morphology, composition and microstructure, and the correspondent, tribological properties of the trivalent chromium composite coatings with carbon nanotubes on the pure aluminum substrate were investigated to explore the wear resistance mechanism of the chromium composite coatings. A crack-bridging bonding model was discussed for the improvement in wear resistance by the carbon nanotubes as reinforced nanometer fiber in the trivalent chromium composite coatings.

2. EXPERIMENTAL SECTION

Pure aluminum plates with an area of $3 \times 3 \text{ cm}^2$ were used as samples substrate. All samples were finely ground through 180, 400, and 800 grit silicon carbide paper. Dimensionally stable mix metal oxide anode of titanium with an area of 12 cm^2 was used to reduce the anodic oxidation of trivalent chromium. Before electroplating, the samples were polished and activated in HNO_3 solution with a concentration of 50 vol. % for 15 s. Due to the oxide films on the aluminum substrate, which

inhibit the direct electroplating of chromium on the substrate, the zincate were used as the interlayer. The zincate protects aluminum against re-oxidation from atmospheric exposure. The zincate layers were deposited from the solution baths composed with sodium hydroxide (250 g/l) and zinc oxide (50 g/l). Electroplating of the trivalent chromium composite coatings was performed from the solution baths composed of $\text{CrCl}_3 \cdot 6\text{H}_2\text{O}$ (200 g/l), HCOOH (32 ml/l), CH_3COOH (10 ml/l), NH_4Cl (30 g/l), KCl (60 g/l), and H_3BO_3 (30 g/l), at a current density of 0.3 A/cm^2 with pH value of 2 at a deposition temperature of 30° C in usual thermo stated glass cell. Deposition time was run for 1 h. In order to provide formation of stable trivalent chromium complexes, a thermal treatment of the chromium bath was carried out at room temperature for 24 h, reaching the reaction in the trivalent chromium bath to thermodynamic equilibrium state. The trivalent chromium composite coatings with adding of MWCNTs (1 g/l) were deposited under ultrasonic agitation with a power of 2 kW with a same deposition time of 1 h. Surface morphology of the trivalent chromium coatings were observed by a Carl Zeiss NTS GMBH-SUPRA55 scanning electron microscopy (FE-SEM). Cross-sectional composition map of the chromium coatings was measured by an SHIMADZU EPMA1600 electron probe micro-analysis (EPMA). Microstructure of the chromium coatings was analyzed by a Panalytical Empyrean x-ray diffractometer with $\text{CuK}\alpha$ radiation. The hardness of the chromium coatings was measured by an HXD-1000TM Vickers microhardness tester with an applied load of 1 N. The indentation measurement was conducted on different area of the chromium coatings with the five measurements to decrease the measurement errors.

Tribological properties were carried out on a WTM-2E tribometer in a ball-on-disc configuration under dry sliding conditions, where the surface of a stationary top-mounted ball was rubbed against a reciprocating sample flat. To eliminate the difference in surface morphology, the two trivalent chromium coatings were polished using 1500 grit silicon carbide paper, and finally cleaned in acetone followed by air drying before the tribological tests. The counterface was a 4 mm-diameter Si_3N_4 ceramic ball using an applied normal load of 0.5-2 N with a relative sliding speed of 0.29 m/s for a sliding distance of 800 m. The friction coefficient was recorded during the wear tests by a transducer on the load arm of the tribometer. Cross-sectional patterns of the wear track were measured using a Surfcoorder KOSAKA ET 4000M profilometer with a $2 \mu\text{m}$ -radius pinhead. The specific wear rate of the samples was calculated per unit sliding distance under unit load, by integrating the area across the wear scar profile through a two-dimensional profile of the track processed using the Origin Pro software, and then multiplying by the circumference length of the track. The surface morphology of the worn samples was identified using the FE-SEM observation.

3. RESULTS

3.1. Morphology and Microstructure

Fig. 1 shows the SEM observation of surface morphology of the trivalent chromium coatings and the trivalent chromium composite coatings with MWCNTs on the pure aluminum substrate with a zincate interlayer, respectively. The trivalent chromium coatings on the aluminum substrate have a

smoother surface with some microcracks [Fig. 1(a) and (b)]. The defects were mainly created by internal stresses generated during the coatings deposition in the trivalent chromium coatings. A few of cracks at the rougher surface of the trivalent chromium composite coatings with MWCNTs were observed [Fig. 1(c)]. The forest network layer of MWCNTs at the surface without the obvious microcracks on the trivalent chromium composite coatings was observed in the larger magnification [Fig. 1(d)]. It is rather remarkable that the carbon nanotubes in the grain boundaries of the chromium composite coatings were different stymies with horizontal [Fig. 1(e) and (f)] and vertical style [Fig. 1(g)]. However, the carbon nanotubes were mainly located with a horizontal style in the grain boundaries of the chromium composite coatings due to the ultrasonic agitation during direct current deposition.

Fig. 2 shows the cross-sectional SEM observation of the trivalent chromium coatings and the trivalent chromium composite coatings with MWCNTs on the pure aluminum substrate with a zincate interlayer, respectively. The two trivalent chromium coatings have a similar thickness of about $35\ \mu\text{m}$ at a current density of $0.3\ \text{A}/\text{cm}^2$ with pH values of 2 at a deposition temperature of $30^\circ\ \text{C}$ for a deposition time of 1 h. A very thin zincate interlayer could not be distinguished due to non-obvious interfaces among the pure aluminum substrate, zincate interlayer, and chromium coating. However, no distinct cracks were observed for the two chromium coatings in the lower magnification.

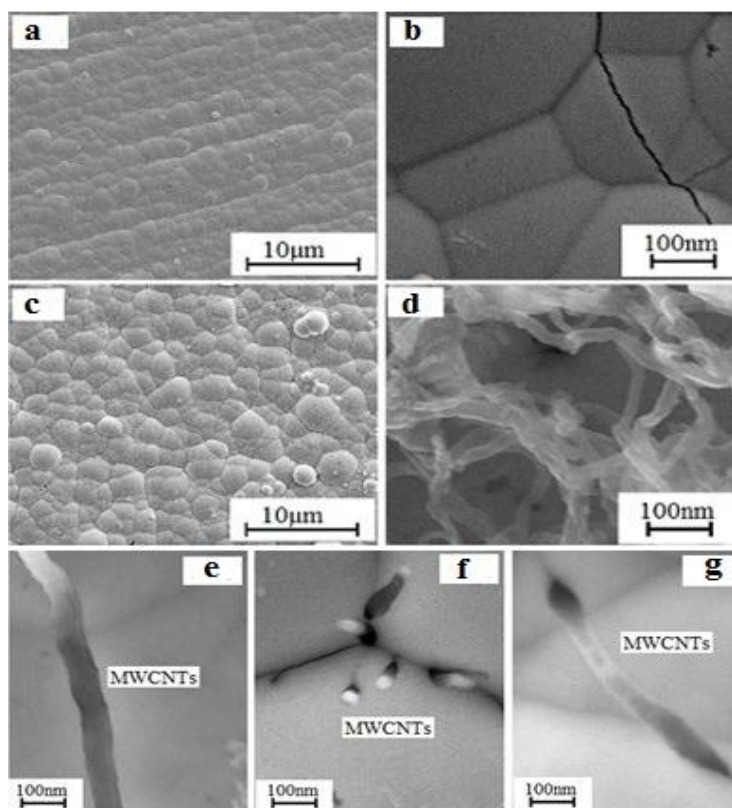


Figure 1. SEM observation of surface morphology of the trivalent chromium coatings [(a) and (b)] and the trivalent chromium composite coatings with MWCNTs [(c)-(g)] on the pure aluminum substrate with a zincate interlayer at a current density of $0.3\ \text{A}/\text{cm}^2$ with pH value of 2 at a deposition temperature of $30^\circ\ \text{C}$, respectively.

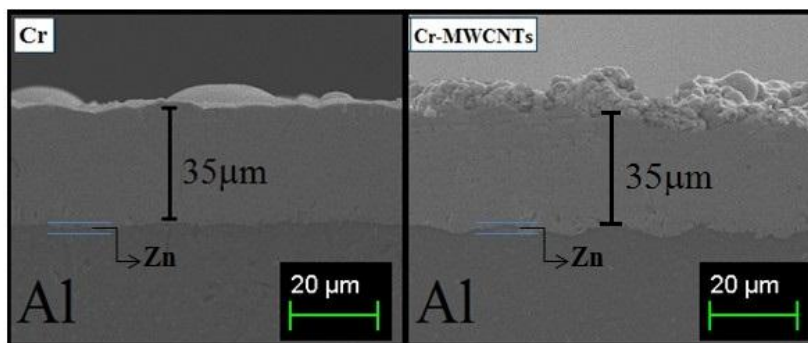


Figure 2. Cross-sectional SEM observation of the trivalent chromium coatings and the trivalent chromium composite coatings with MWCNTs on the pure aluminum substrate with a zincates interlayer, respectively.

Fig. 3 shows the EPMA composition map for the cross-section of the trivalent chromium composite coatings with MWCNTs on the pure aluminum substrate with a zincate interlayer. The carbon nanotubes have a high concentration in the grain boundaries of the chromium composite coatings than that inside the chromium grains. A thin and continue zincate interlayer about 2 μm thick was obviously observed between the pure aluminum substrate and chromium coating. A high density of carbon nanotubes existed near the zincate interlayer due to a high primary deposition rate during a starting time of several minutes. The specification of carbon nanotubes such as length and diameters and the deposition conditions such as deposition temperature, pH value, and ultrasonic agitation conditions were effective on dispersion of carbon nanotubes [10, 14].

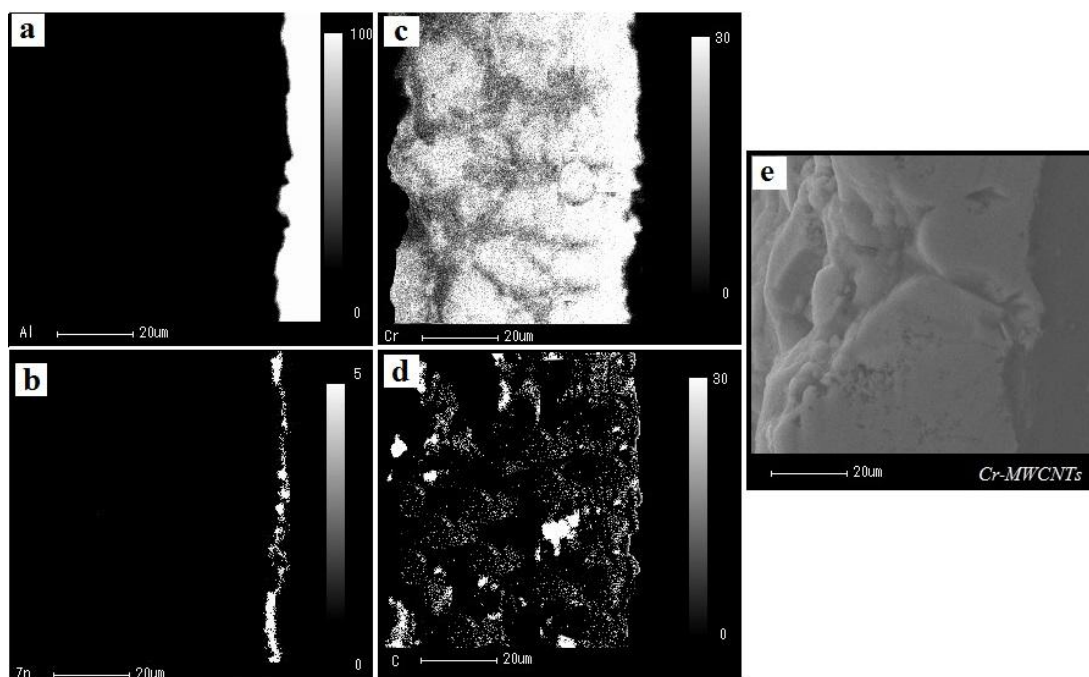


Figure 3. EPMA composition map for the cross-section of the trivalent chromium composite coatings with MWCNTs on the pure aluminum substrate with a zincate interlayer

Fig. 4 shows the XRD patterns of the trivalent chromium coatings and the trivalent chromium composite coatings with MWCNTs on the pure aluminum substrate with a zincate interlayer, respectively. A typical amorphous structure with a limited crystallization was observed for the two trivalent chromium coatings. A diffraction peak (002) of carbon was detected from the carbon nanotubes in the trivalent chromium composite coatings. Recently, Protsenko et al. [15] reported that the trivalent chromium coatings had either amorphous or a nanocrystalline microstructure from an aqueous sulfate trivalent chromium bath. Ghaziof et al. [16] also found that the crystalline or amorphous structure of the trivalent chromium coatings was independent on the surface morphology and grain size of the coatings. With a current density from 0.3 to 0.4 A/cm² at a deposition temperature of 30-35° C, the crystallization degree of the trivalent chromium coatings has no apparent change, which was similar to that observed that from the trivalent chromium bath containing carbamide and formic acid [15, 17].

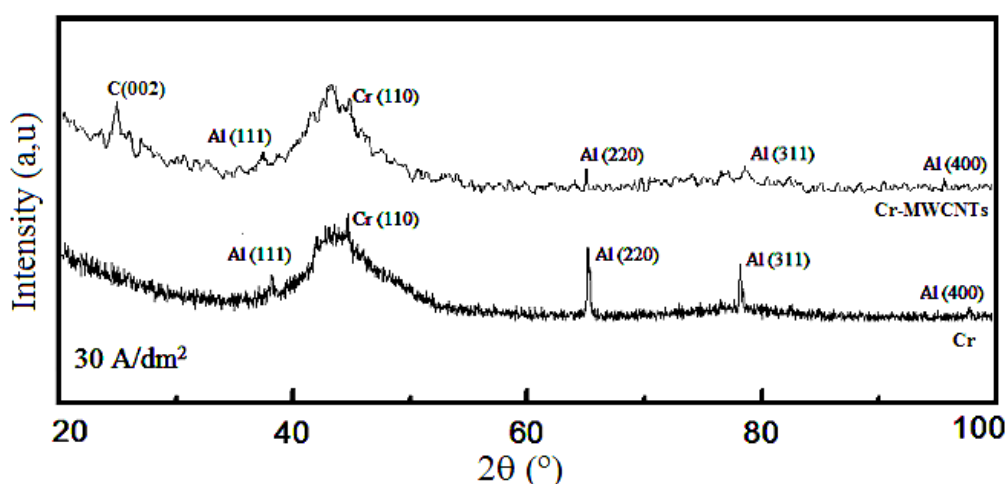


Figure 4. XRD patterns of the trivalent chromium coatings and the trivalent chromium composite coatings with MWCNTs on the pure aluminum substrate with a zincates interlayer, respectively.

3.2. Hardness

Fig. 5 shows the microhardness of the trivalent chromium coatings and chromium composite coatings with MWCNTs on the pure aluminum substrate with a zincate interlayer, compared with that of the pure aluminum substrate. The microhardness of the pure aluminum substrate was HV_{1 N} 0.6-0.7 GPa. A typical microhardness of the trivalent chromium coatings was detected on the pure aluminum substrate as HV_{1 N} 8.0-8.3 GPa. The chromium composite coatings reinforced by the carbon nanotubes slightly increased the microhardness to HV_{1 N} 9.2-9.8 GPa. It is a note that the carbon nanotubes have a limited reinforcement effect in hardness on the trivalent chromium coatings, unlike to the reinforcement fibers in the metallic matrix composites using carbon nanotubes [18, 19].

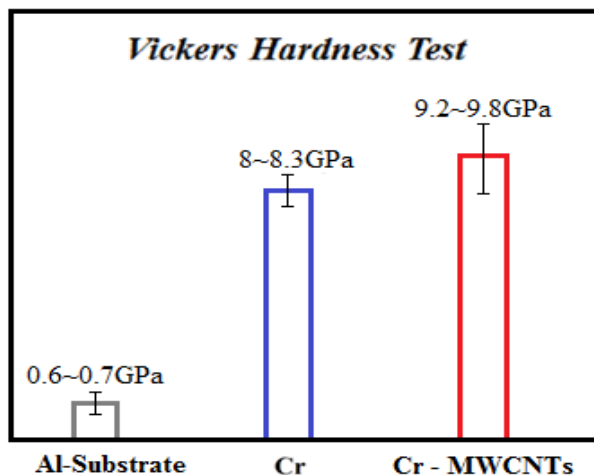


Figure 5. Microhardness of the trivalent chromium coatings and chromium composite coatings with MWCNTs on the pure aluminum substrate with a zincate interlayer, compared with that of the pure aluminum substrate.

3.3. Tribological Properties

Wear resistance for the pure aluminum had the large plastic strain at the subsurface of the sliding pin as mentioned in previous research [20]. The subsurface cracks are induced due to the repeated plastic deformation between the test pin and disc. In the aluminum wear test results shows in the dry sliding process, the plastic agglomerates into spheres that were removed by the next slider. Hardness and friction coefficient will play a major role in the overall wear process. In compare the trivalent chromium and chromium composite coatings had hard surfaces. The chromium electroplating plays an important role to increase the mechanical properties of the aluminum surfaces.

Fig. 6 shows the friction coefficients of the trivalent chromium coatings and the chromium composite coatings with MWCNTs on the pure aluminum substrate with a zincate interlayer under a normal load of 0.5-2 N, respectively. A distinct peak of the friction coefficients was detected in the starting sliding time for the two trivalent chromium coatings. A relative long running-in duration was also detected at the lower normal loads for the trivalent chromium coatings.

The stable friction coefficients were obtained during the longer sliding time for the two trivalent chromium coatings. At a lower normal load of 0.5 N, the higher friction coefficients of about 0.60 and 0.57 were detected for the trivalent chromium coatings and the chromium composite coatings with MWCNTs, respectively. With increasing the normal load to 1 N, a similar friction coefficient of about 0.60 to that at 0.5 N was obtained for the chromium composite coatings, and a lower friction coefficient of about 0.55 for the pure trivalent chromium coatings. At a higher normal load of 2 N, the decreased friction coefficients to about 0.50 and 0.47 were detected for the trivalent chromium coatings and the chromium composite coatings with MWCNTs, respectively.

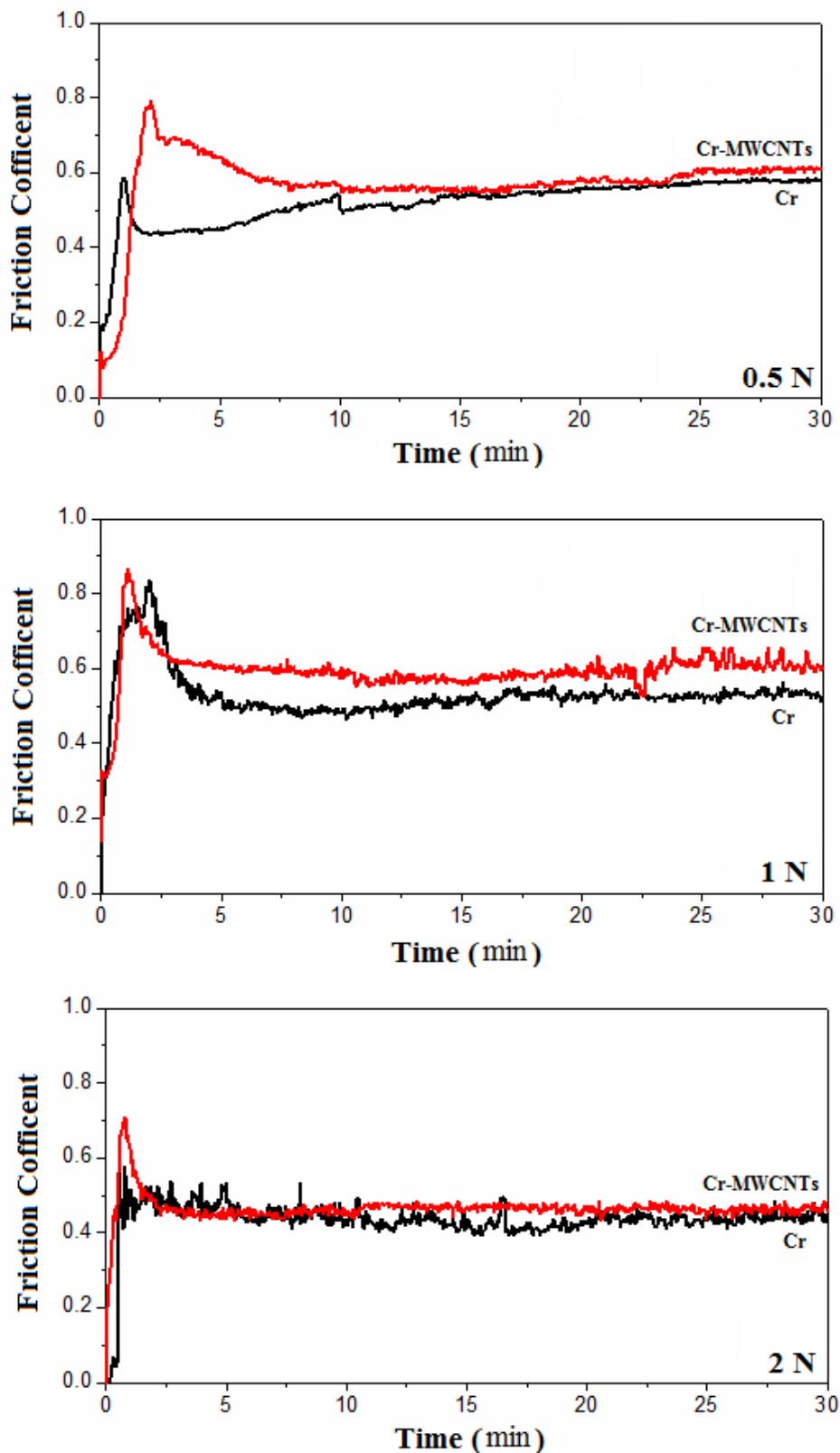


Figure 6. Friction coefficients of the trivalent chromium coatings and the chromium composite coatings with MWCNTs on the pure aluminum substrate with a zincate interlayer under a normal load of 0.5-2 N, respectively.

Fig. 7 shows the specific wear rate of the trivalent chromium coatings and the chromium composite coatings with MWCNTs on the pure aluminum substrate with a zincate interlayer under normal loads of 0.5-2 N, respectively. For the trivalent chromium coatings, the specific wear rate was obtained as 2.63×10^{-7} , 3.34×10^{-7} , and 4.43×10^{-7} mm³/Nm with the applied normal loads of 0.5, 1, and 2 N, respectively.

The decreased specific wear rate of the trivalent chromium composite coatings with MWCNTs was correspondently as 1.84×10^{-7} , 2.32×10^{-7} and 2.74×10^{-7} mm³/N m, respectively. At the lower normal loads of 0.5 and 1 N, the wear resistance of the chromium composite coatings increased by about 30 %, compared with that the pure chromium coatings. When the normal load increased to 2 N, the increase in were resistance of the chromium composite coatings was achieved by about 40 %.

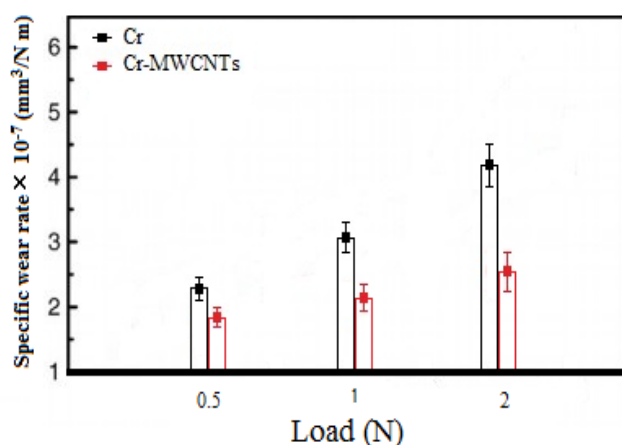


Figure 7. Specific wear rate of the trivalent chromium coatings and the chromium composite coatings with MWCNTs on the pure aluminum substrate with a zincate interlayer under normal loads of 0.5 to 2 N.

Fig. 8 shows the typical SEM morphologies of worn surfaces for the trivalent chromium coatings and chromium composite coatings with MWCNTs on the pure aluminum substrate with a zincate interlayer under a normal load from 0.5 to 2 N, respectively. At a lower normal load of 0.5 N, a slight abrasive and adhesive wear mode were observed for the two trivalent chromium coatings. A few plate-like debris formed on the chromium composite coatings with MWCNT [Fig. 8(b)], compared with that on the trivalent chromium coatings [Fig. 8(a)]. The two chromium composite coatings was HV_{1 N} 8.0-8.3 GPa and 9.2-9.8 GPa in hardness and the Si₃N₄ ceramic as a counterface material had HV 15.7 GPa, their specific wear rates of 2.63×10^{-7} and 1.84×10^{-7} mm³/N m respectively between the two hard solids was attributed to plastic flow of the trivalent chromium coatings in the dry contact with the harder Si₃N₄ ceramic. The accumulation of plate-like debris composed of MWCNTs was also observed for the chromium composite coatings [Fig. 8(c)].

When the normal load increased to 1 N, a mild abrasive and adhesive wear mode was observed for the two trivalent chromium coatings. The high mechanical interaction between the trivalent chromium coatings and Si₃N₄ ceramic was attained with the distinct sticking and cracking [Fig. 8(d)]. However, the shallow plastic prows with the smaller plate-like debris formed during the sliding for the

chromium composite coatings, corresponding to a specific wear rate of $2.32 \times 10^{-7} \text{ mm}^3/\text{N m}$. [Fig. 8(e)]. The significant plastic flow of the trivalent chromium coatings was detected with the specific wear rate of $3.34 \times 10^{-7} \text{ mm}^3/\text{N m}$. [Fig. 8(d)]. The forest network of carbon nanotubes was also found on the worn surface for the chromium composite coatings [Fig. 8(f)].

At a higher normal load of 2 N, the different wear modes were obtained for the two trivalent chromium coatings. The severe adhesive and abrasive wear mode from the surface oxidation process with the specific wear rate of $4.43 \times 10^{-7} \text{ mm}^3/\text{Nm}$ was observed due to the mechanically mixed chromium oxides particles for the trivalent chromium coatings [Fig. 8(g)]. Otherwise, the mild abrasive wear mode was observed with the specific wear rate of $2.74 \times 10^{-7} \text{ mm}^3/\text{N m}$ between the metallic and non-metallic solids for the chromium composite coatings [Fig. 8(h)]. The metallic particles with the small oxides debris formed within the valleys of plastic flows on the worn surface for the chromium composite coatings [Fig. 8(i)]. The more stable friction coefficients of the chromium composite coatings may contribute to the lubrication from the carbon nanotubes at the worn surface.

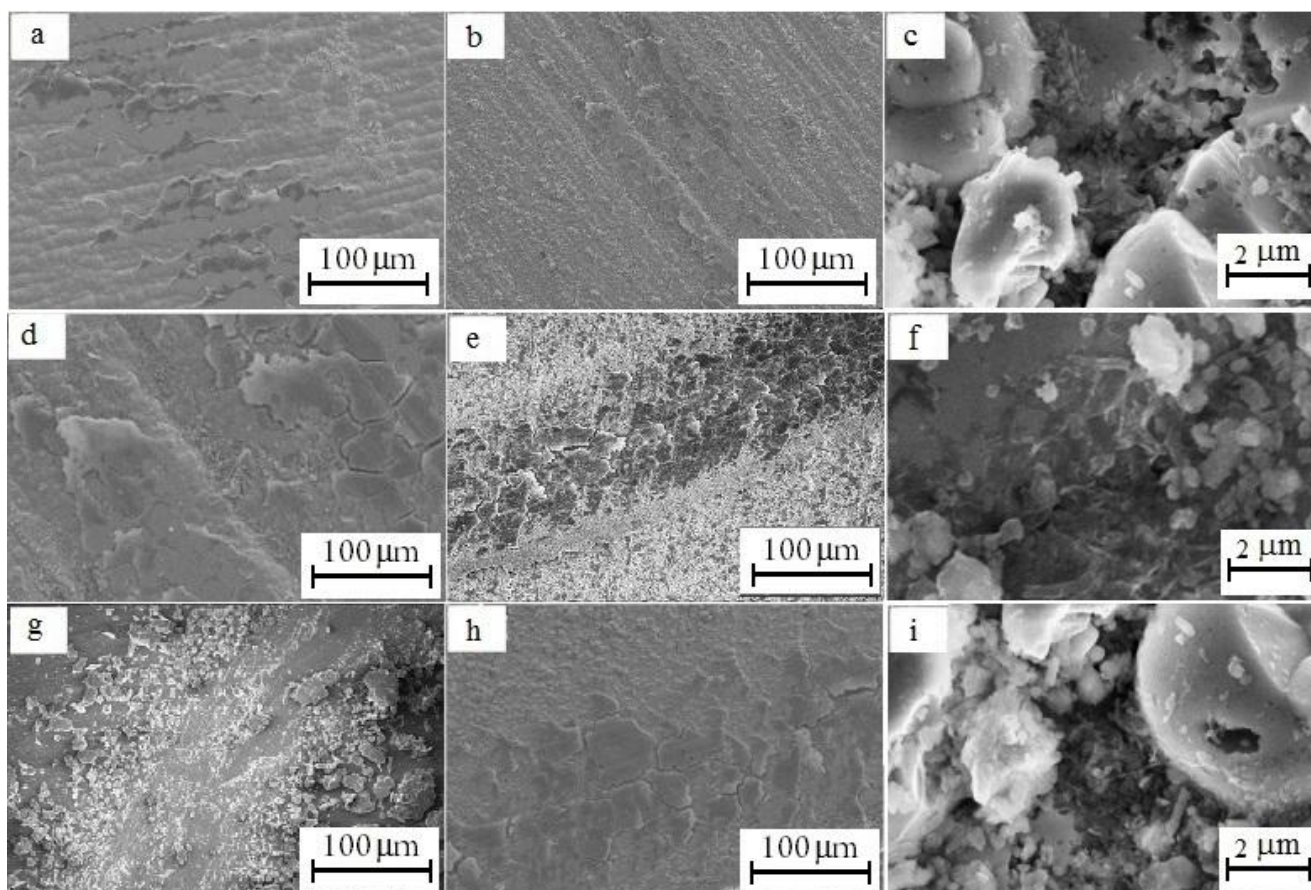


Figure 8. Typical SEM morphologies of worn surfaces for the trivalent chromium coatings [(a), (d), (g)] and chromium composite coatings with MWCNTs [(b), (c), (e), (f), (h), and (i)] on the pure aluminum substrate with a zincate interlayer under a normal load of 0.5 N, 1 N and 2 N respectively.

4. DISCUSSION

The carbon nanotubes as reinforced nanometer fiber in the chromium composites coatings exhibited the increased mechanical properties, such as higher hardness and improved wear resistance. Comparing the microhardness of the trivalent chromium composite coatings, their wear properties showed a more improvement, because the carbon nanotubes located through the chromium grains just improved the mechanical properties with a novel reinforcement mechanism. When the carbon nanotubes were the horizontal stymies, the two chromium grains were bonding together through the carbon nanotubes with reinforcement. The bridging effect was increased the bonding of the two chromium grains. The carbon nanotubes prevented generation of the cracks in the composite coatings matrix. The intrinsic defects of the trivalent chromium coatings could be bridging during the direct current deposition. Unlike the reinforcement mechanism of carbon nanotubes in the metallic and ceramic composites [18, 19], the increase in the mechanical properties of the chromium composite coatings with MWCNTs was dependent on the crack-bridging bonding [10].

Fig. 9 shows the schematic image of a crack-bridging bonding model using the carbon nanotubes in the trivalent chromium coatings, and the typical SEM morphologies on the bridging zones with the carbon nanotubes in the chromium grains boundaries, respectively. The carbon nanotubes with the crack-bridging bonding and grains bonding increased the strength of chromium grains jointing specially in the grain boundaries [Fig. 9(a)]. The crack-bridging bonding was as an important source of toughening in the chromium composite coatings. During the sliding, the microcracks were piled up as encountered behind the carbon nanotubes with the promulgation in the chromium composite coatings. When the stress in the crack and/or grain boundaries increased much more than carbon nanotubes resistance, the cracks opening happened and a severe cracks growth led to cross fracture in the chromium composite coatings [Fig. 9(b)]. When the bridging zone was larger than the size and spacing of the discrete crack elements, the bridging tractions may be approximated by a continuous pressure [Fig. 9(c)]. If the crack front passed the trap site without rupturing the carbon nanotubes or the interfacial bond, then a complete bridge was left behind. This carbon nanotubes bridge has the action as a spring exerting a closing pressure on the crack flanks [Fig. 9(d)]. The resulting reduction of the crack driving force led to an additional toughening effect. An array of nonlinear springs were joint the two sides of cracks and two halves of a chromium grains body. The springs right at the tip of the crack deformed more during the sliding, but the springs far ahead the tip of the crack deformed negligibly. The deformation in the springs was inhomogeneous at the chromium grains boundaries. The long horizontal nanotubes can make better reinforcement and increase the bonding of the chromium grains in the composite coatings. The location of the carbon nanotubes in the chromium grain boundaries might be having the sufficient effects on improvement of mechanical properties in the chromium composite coatings. In contrary, when carbon nanotubes presented in the vertical style as the same as place the same position on the grain boundaries, the negative effects caused the increase in the cracks in chromium grain boundaries. The vertical carbon nanotubes increased the internal stress in the chromium grain boundaries and had the similar effect like impurity defects and negatively source of cracks generation. It was found that the ultrasonic agitation played an important role in vertical and horizontal style of carbon nanotubes stymies for the trivalent chromium

composite coatings. The horizontal stymies of carbon nanotubes were obtained in the trivalent chromium composite coatings with MWCNTs.

The crack-bridging bonding model was proposed for the toughening of a discontinuous fiber-reinforced in matrix composite, in which the frictional bridging of fibers during, as well as after, the interfacial debonding was considered. Vashishth et al. [21] observed the effect of carbon nanotubes as the barrier in the damage-zone of the cracks in bio-composite materials. The nanotubes acted as an impediment in microcracking zone and the resultant dilation of cracks growth in this zone, which was constrained by the surrounding rigid material can act to shield the crack tip and hence, extrinsically toughen the material. Similar reports on the amorphous ceramic coatings showed that introduction of the carbon nanotubes into the composite coatings was an effective way to increase the hardness and toughness, because it brought the two-phase boundaries and inhibited the promulgation of cracks [22]. Dong et al. [18] showed that owing to the carbon nanotubes in the Cu composite coatings, the fracture induced by cracks was reduced in the Cu-nanotube composite, and the cracks was more difficulty propagation, due to flaking and piled up as encountered the carbon nanotubes during the sliding. Therefore, the crack-bridging bonding model was reasonably used to explore the improvement mechanism in wear resistance by the carbon nanotubes as reinforced fiber in the trivalent chromium composite coatings.

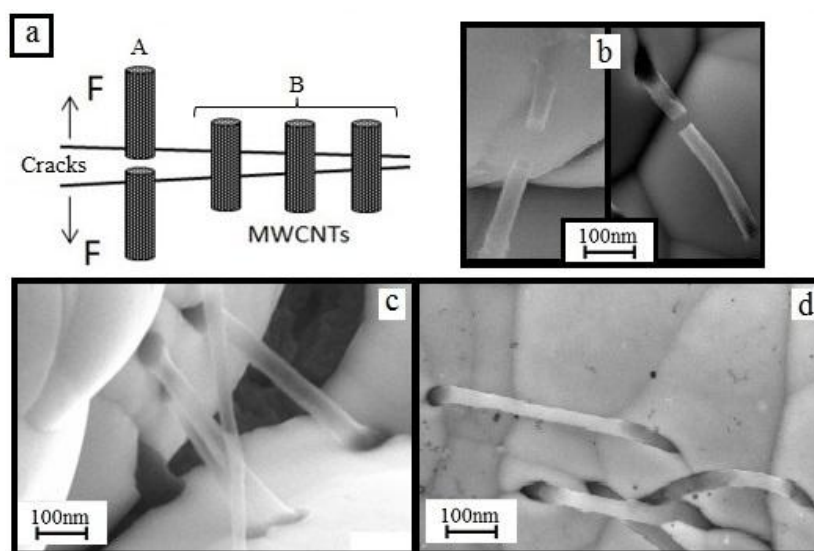


Figure 9. Crack-bridging bonding model using the carbon nanotubes in the trivalent chromium coatings: Schematic image (a); SEM observation of bridging zones [(b)-(d)].

5. CONCLUSIONS

(1) The trivalent chromium composite coatings about 35 μm thick with MWCNTs were fabricated by the direct current deposition at a current density of 0.3 A/cm^2 with pH value of 2 at a deposition temperature of 30° C with the MWCNTs adding of (1 g/l) under an ultrasonic agitation with

a power of 2 kW during a deposition time of 1 h on the pure aluminum substrate using a zincate interlayer of about 2 μm thickness.

(2) The chromium composite coatings with MWCNTs have the similar amorphous microstructure with a limited crystallization to that for the pure trivalent chromium coatings. The microhardness of the chromium composite coatings slightly increased to $\text{HV}_{1\text{N}} 9.2\text{-}9.8\text{ GPa}$ from $\text{HV}_{1\text{N}} 8.0\text{-}8.3\text{ GPa}$ of the pure chromium coatings.

(3) The two trivalent chromium coatings possessed the similar friction coefficient changed in 0.60-0.47 under the applied normal load of 0.5-2 N. The significant increase in the wear resistance of the chromium composite coatings with MWCNTs was found with the specific wear rate decreased by about 30-40 % under the applied normal load, compared with that of the pure chromium coatings.

(4) A crack-bridging bonding model was proposed to explore the improvement mechanism in wear resistance by the carbon nanotubes as reinforced nanometer fiber in the trivalent chromium composite coatings. The long horizontal nanotubes in the chromium grain boundaries can make better reinforcement and increase the bonding of the chromium grains in the chromium composite coatings.

ACKNOWLEDGEMENT

We acknowledge contributory discussions and technical assistant of W. Zhang, S. Tong in this research. This work is supported by the National Basic Research Program of China under Grant no. 2009CB724305. One author (E. Khodadad) gratefully acknowledges Chinese Scholarship Council (CSC), China, for the financial support.

References

1. L. Fedrizzi, S. Rossi, F. Bellei, and F. Deflorian, *Wear*, 253 (2002) 1173.
2. J. De Mello, J. Gonçalves Jr, and H. Costa, *Wear*, 302 (2013) 1295.
3. E. Khodadad and M. Lei, *Int. J. Electrochem. Sci*, 9 (2014) 1250.
4. X. Dong, P. Wang, S. Argekar, and D. W. Schaefer, *Langmuir*, 26 (2010) 10833.
5. C. Fontanesi, R. Giovanardi, M. Cannio, and E. Soragni, *J. Appl. Electrochem.*, 38 (2008) 425.
6. R. Giovanardi and G. Orlando, *Surf. Coat. Technol.*, 205 (2011) 3947.
7. Z. Zeng, L. Wang, A. Liang, and J. Zhang, *Electrochim. Acta*, 52 (2006) 1366.
8. A. Liang, L. Ni, Q. Liu, and J. Zhang, *Surf. Coat. Technol.*, 218 (2012) 23.
9. V. Protsenko, V. Gordiienko, F. Danilov, and S. Kwon, *J. Chem.*, 8 (2011) 1925.
10. J. N. Coleman, U. Khan, W. J. Blau, and Y. K. Gun'ko, *Carbon*, 44 (2006) 1624.
11. Z. Zeng, Y. Zhou, B. Zhang, Y. Sun, and J. Zhang, *Acta Mater.*, 57 (2009) 5342.
12. L. Bin, Z. Zeng, and Y. Lin, *Surf. Coat. Technol.*, 203 (2009) 3610.
13. Z. Zeng, Y. Yu, and J. Zhang, *J. Electrochem. Soc.*, 156 (2009) 123.
14. M. Deng, G. Ding, Y. Wang, X. Cui, H. Wang, F. Zang, and H. Wu, *Vacuum*, 85 (2011) 827.
15. V. Protsenko, F. Danilov, V. Gordiienko, S. Kwon, and M. Kim, *Thin Solid Films*, 520 (2011) 380.
16. S. Ghaziof, M. Golozar, and K. Raeissi, *J. Alloys Compd.*, 496 (2010) 164.
17. V. Protsenko, F. Danilov, V. Gordiienko, and A. Baskevich, *Int. J. Refract. Met. Hard Mater.*, 31 (2012) 281.
18. S. Dong, J. Tu, and X. Zhang, *Mat. Sci. Eng., A*, 313 (2001) 83.
19. M. M. Bastwros, A. M. Esawi, and A. Wifi, *Wear*, 307 (2013) 164.
20. A. Prasada Rao, K. Das, B. Murty, and M. Chakraborty, *Wear*, 264 (2008) 638.
21. D. Vashishth, K. Tanner, and W. Bonfield, *J. Biomech.*, 36 (2003) 121.

22. A. L. Vasiliev, R. Poyato, and N. P. Padture, *Scripta Mater.*, 56 (2007) 461.

© 2014 The Authors. Published by ESG (www.electrochemsci.org). This article is an open access article distributed under the terms and conditions of the Creative Commons Attribution license (<http://creativecommons.org/licenses/by/4.0/>).